RESULTS OF THE MARS SUBSURFACE WATER ICE MAPPING (SWIM) PROJECT. N. E. Putzig,[1] G. A. Morgan,[1] H. G. Sizemore,[1] D. M. H. Baker,[2] A. M. Bramson,[3] E. I. Petersen,[3] Z. M. Bain,[1] R. H. Hoover,[4] M. R. Perry,[1] M. Mastrogiuseppe,[5] I. B. Smith,[1] B. A. Campbell,[6] A. V. Pathare,[1] C. M. Dundas.[7] [1]Planetary Science Institute: nathaniel@putzig.com, [2] NASA Goddard Space Flight Center, [3]University of Arizona,[4]Southwest Research Institute, [5]California Institute of Technology, [6]Smithsonian Institution, [7]USGS, Astrogeology Science Center.

Introduction: In the effort to deliver humans to the surface of Mars and returning them safely to Earth, current propulsion technology means that mass represents the ultimate premium for cost. Thus, any such endeavor must leverage all available *in situ* resources. The most valuable Martian resource for "living off the land" is water, which when combined with atmospheric carbon dioxide, can provide methane as a fuel to sustain an outpost and for the return to Earth. Water also represents one of the most important ingredients of life support, including as a source of oxygen for breathing.

Mars has plentiful surface water ice, with two kilometers-thick ice caps in the form of the north and south polar layered deposits and widespread shallow (<1 m depth) high-latitude ground ice. However, these sources of water are at latitudes that are not feasible for the first human missions to the Red Planet. The higher solar radiation and manageable length of night offered by the lower latitudes are valuable to mission success, and low latitudes reduce launch energy. Thus, future mission planning must isolate regions of Mars that optimize both water sources and solar energy supplies.

Ice Resources on Mars: Non-polar ice that is accessible in the scope of most mission architectures (i.e., within the upper few meters) has been discovered on Mars through remote sensing. For example, fresh impacts revealing icy substrate have been reported using HiRISE data [1-2] and glacial deposits have been found in the mid-latitudes with geomorphologic and radar sounding studies [e.g., 3]. Knowledge of the complete inventory of the distribution and depth range of these water ice deposits across Mars is therefore of enormous value to human missions.

The SWIM Project: The primary goal of this project is to generate ice mapping products to enable future mission planning. Previously, global studies of Martian ice deposits have been science-driven and largely concentrated on one or two data types, such as neutron maps [4] and geomorphic surveys of periglacial features [e.g. 5].

The SWIM project is unique in that it integrates all appropriate orbital datasets to provide a holistic assessment of accessible Martian ice reserves. By employing a team with a diverse background of relevant expertise and by leveraging new data processing techniques, the SWIM Project has generated the most up-to-date maps of Martian water ice distribution. To date, the project has included global reconnaissance mapping with thermal and radar data as well as focused multi-dataset mapping between 0º and 60ºN within the majority of the northern hemisphere (everywhere apart from 225°E to 290°E) to characterize the distribution of water ice (Fig 1). Placing the primary focus of this study in the northern hemisphere was driven by the broader availability of preferred landing conditions at lower elevations (i.e., higher atmospheric density) relative to most areas in the southern hemisphere.

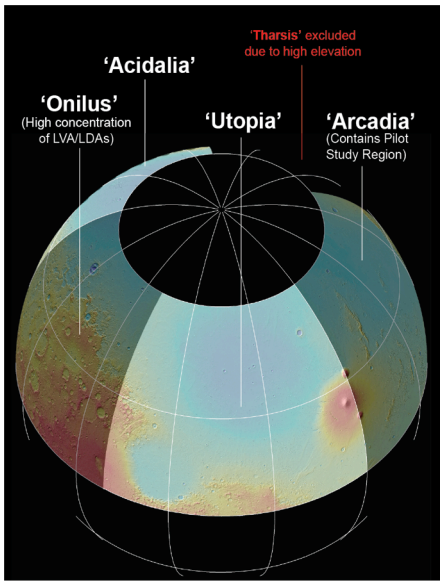

Figure 1. *Four SWIM study regions encompass much of the Martian northern hemisphere.*

Methods: To search for and assess the presence of shallow ice across our study regions, the SWIM project uses the following techniques and datasets: neutron-detected hydrogen (MONS), thermal behavior (both TES and THEMIS), multi-scale geomorphology (HiRISE, CTX, HRSC, and MOLA), and radar surface and subsurface echoes (SHARAD). To extract the maximum amount of information from the datasets, we employ newly developed techniques, including: super-resolution (bandwidth-extrapolation) radar processing, which can improve the range resolution by up to a factor of 3 [6], surface radar reflectivity [7], and refined thermal modeling [8] along with more traditional approaches to geomorphological mapping [9] and interpretation of discrete radar-detected subsurface interfaces [10].

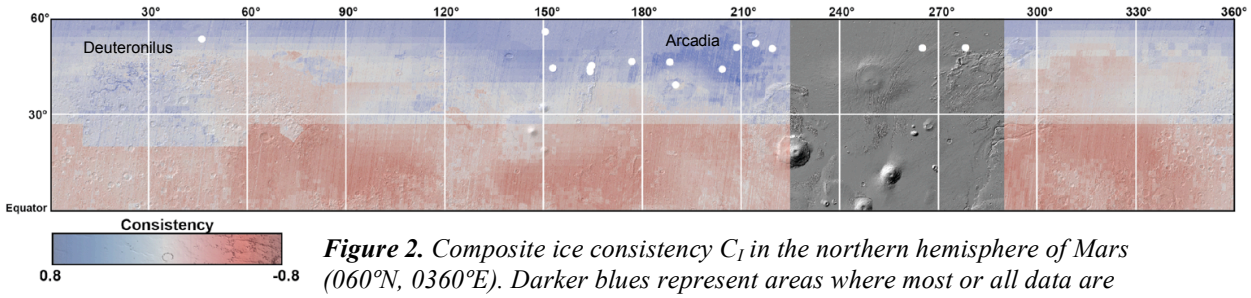

Figure 2. *Composite ice consistency C_I in the northern hemisphere of Mars (060ºN, 0360ºE). Darker blues represent areas where most or all data are consistent with the presence of buried ice. Locations of fresh ice-exposing impacts [2] are shown as white dots, and they occur on blue pixels within the SWIM study region. Areas between 225ºE and 290ºE were omitted from the study due to high elevations deemed inaccessible for human missions.*

Each of the above datasets probes to different depths into the subsurface. To enable a quantitative assessment of how consistent (or inconsistent) the various remote sensing datasets are with the presence of shallow (<5 m) and deep (>5 m) ice across our study regions, we introduced the SWIM Equation:

$$C_I = (C_N + C_T + C_G + C_{RS} + C_{RD}) / 5$$

Ice consistency values C_X range between -1 and +1, where -1 means that the data are inconsistent with the presence of ice, 0 means that the data give no indication of the presence or absence of ice, and +1 means that the data are consistent with the presence of ice. In the SWIM Equation, we calculate a composite ice consistency C_I for each pixel of our map by summing each individual consistency value (C_N for neutron data, C_T for thermal data, C_G for geomorphic data, C_{RS} for radar surface-return data, and C_{RD} for radar subsurface dielectric-constant data) and normalizing by the number of datasets [11]. This formulation gives equal weight to all inputs and indicates the consistency of the data sets, but does not directly correspond to a probability that ice is present. Future revisions of the equation may include the use of different weightings.

Results: In Fig. 2, we display a composite ice consistency map derived from our multi-dataset analysis, which spans the entire study region in the northern hemisphere of Mars. The highest consistency values, which are indicative of multiple individual datasets reporting positive (blue) ice signatures, typically occur poleward of ~40ºN—notably in Arcadia Planitia where previous work found indications of widespread ground ice [12] and in Deuteronilus Mensae where others have mapped extensive debris-covered glaciers [13]—but many positive (blue) values extend to southward to as low as ~20ºN. In most areas equatorward of 28ºN, the integrated map displays negative (red) values, arguing for ice-free conditions at these lower latitudes.

At the 9th International Conference on Mars, we will provide an overview of the entire project and present the full results of our ice mapping efforts. These new mapping products represent valuable tools for mission planning activities, and they will directly support the next Human Landing Site Selection Workshop. Beyond human mission planning, SWIM results will highlight limitations of our previous and current orbital assets, providing a framework to advise the next generation of robotic missions. Broader scientific findings that may stem from this effort will be presented by Morgan et al. [this conference].

To Learn More: For more information on the SWIM project, GIS-ready map products, and news of the latest releases, visit https://swim.psi.edu and follow us on Twitter @RedPlanetSWIM.

Acknowledgements: The SWIM project is supported by NASA through JPL Subcontract 1611855. PSI is grateful to SeisWare International Inc. for academic licensing of their Geophysics software that is used in our radar analysis.

References: [1] Byrne S. et al. (2009) Science 325, 1674-1676. [2] Dundas C.M. et al. (2014) Geophys. Res. Lett. 119, 109-127. [3] Holt, J. Science, 322, 1235-1238. [4] Feldman, W. C., Science, 297, 75-78. [5] Head, J. et al., Nature, 426, 797 - 802. [6] Raguso M.C. et al. (2018) 5th IEEE Int. Wkshp Metrology for Aerospace. [7] Bain Z.M. et al. (2019) Lunar. Planet. Sci. Abs. 2726. [8] Hoover, R. et al. (2019) Lunar. Planet. Sci. Abs. 1679. [9] Putzig N.E. et al. (2019) Lunar. Planet. Sci. Abs. 2087. [10] Bramson A.M. et al. (2019) Lunar. Planet. Sci. Abs. 2069. [11] Perry M.R. et al. (2019) Lunar. Planet. Sci. Abs. 3083. [12] Bramson A.M. et al. (2015) GRL 42, 6566-6574. [13] Petersen E.I. et al. (2018) GRL 45, 11,595-11,604.